THE ASTROPHYSICAL JOURNAL, 405:307–311, 1993 March 1

BINARY STRUCTURE AND ACCRETION FLOW OF THE NEW INTERMEDIATE POLAR H0253+193

YUICHI KAMATA
Department of Astrophysics, School of Science, Nagoya University, Furo-cho, Chikusa-ku, Nagoya 464-01, Japan
AND
KATSUJI KOYAMA
Department of Physics, Faculty of Science, Kyoto University, Sakyo-ku, Kyoto 606-01, Japan
Received 1992 April 23; accepted 1992 September 9

ABSTRACT

This paper describes X-ray spectral variations of H0253+193 during its 6 hr binary orbit and 206 s pulsation. The orbital-phase–resolved X-ray spectra were well fitted by a thermal bremsstrahlung model with a temperature ranging from 16 to 33 keV and an iron emission line at about 6.7 keV. No systematic change of the temperature with orbital phase was found, but a clear orbital modulation of the hydrogen column density (N_H) was discovered. H0253+193 shows total eclipses and double-peaked pulse profiles. During the ingress and egress of the eclipse, no significant spectral change was observed. The fractional pulse amplitude decreases as the X-ray energy increases. A possible geometry of the binary system and the structure of the accretion flow are discussed.

Subject headings: binaries: close — stars: individual (H0253+193) — X-rays: stars

1. INTRODUCTION

The X-ray source H0253+193 was discovered by the *Einstein* Imaging Proportional Counter (IPC) measurement at the center of the dark cloud Lynds 1457, the nearest molecular cloud with a distance of 65 pc (Hobbs, Blitz, & Magnani 1986), also known as MBM 12 (Magnani, Blitz, & Mundy 1985). From this positional coincidence, H0253+193 was first interpreted to be an X-ray–emitting protostar in the dense molecular cloud (Halpern & Patterson 1987; Takano, Koyama, & Makishima 1989a). Other possibilities such as an RS CVn star were also discussed (Clemens & Leach 1989).

From *Ginga* observations made in 1987 and 1988, a coherent X-ray pulsation was discovered with a period of approximately 206 s (Takano et al. 1989b; Koyama et al. 1991). Since this period was found to be very stable, H0253+193 was considered to contain a strongly magnetized compact object with a spin period of 206 s. Thus one possibility was that H0253+193 is an isolated compact object powered by the gas accretion from the ambient molecular cloud MBM 12. However, the hydrogen column density toward MBM 12 determined by radio observations is only 1.4×10^{22} cm^{-2}, while that determined by the X-ray spectrum of H0253+193 is as large as 10^{23} cm^{-2} and is variable in time (Koyama et al. 1991). Therefore, it is doubtful that H0253+193 is really associated with the molecular cloud MBM 12. Patterson & Halpern (1990) extensively discussed the nature of this source and pointed out that the observed nature resembles that of white dwarf binaries rather than isolated compact objects. They suggested that H0253+193 is likely to be a DQ Herculis type of cataclysmic variable or an intermediate polar (IP), a class of white dwarf binary.[1]

Since dust extinction in the optical band is very high, a search for an optical counterpart was realistic only in the near-infrared band. Koyama et al. (1991) have found one IR object in the error region of H0253+193 with a K-magnitude value of 13.5 ± 0.1. The K-magnitude value and the X-ray luminosity of H0253+193 are well explained if this object is an IP behind the dark cloud.

Recently Kamata, Tawara, & Koyama (1991, hereafter Paper I) discovered 6 hr periodic eclipses in the X-ray light curve of H0253+193. The 206 s pulsation and 6 hr orbital period are typical values for IPs. The sizes of the compact star and its optical companion are estimated from the duration and transition time of the eclipse, and are consistent with a white dwarf and a late-type star, respectively. The X-ray spectrum of H0253+193 fits a model of thermal bremsstrahlung with a temperature of about 30 keV with a 6.7 keV iron line, which is typical of white dwarf binaries rather than neutron star binaries.

Thus the likelihood that H0253+193 is a new IP can be established, although no information from optical spectroscopy is available. A short report on the discovery of the periodic eclipse and a brief discussion are found in Paper I. In the present paper we discuss the binary structure and accretion flow of the new IP H0253+193, on the basis of the analysis of orbital- and pulse-phase–resolved spectra.

Brief descriptions of the instruments and this observation are indicated in § 2. In § 3 we show the results on source position from the scanning observation, orbital variation of the X-ray spectra, spectral variation near observed eclipses, and the pulse profiles. In § 4 we discuss binary parameters and the structure of the accretion flow onto the magnetic white dwarf. In § 5 we summarize the results and discussion.

2. OBSERVATIONS

The *Ginga* observations were made with the Large Area Proportional Counter (LAC), which has a 2–37 keV energy band and a maximum effective area of 4000 cm^2. Details of the

[1] Stars of DQ Her type with longer pulse periods (>100 s) are sometimes called intermediate polars (IPs). Unlike IPs, the shorter period stars tend to be only weak X-ray sources. Thus the 206 s X-ray pulsator H0253+193 may lie between these two classes. In this paper we join these into a single class (see Patterson & Halpern 1990).

TABLE 1

OBSERVATION LOG

Date 1989 August	Observations
10 (16:30)–10 (18:30).....	Scan (path A)
10 (19:00)–11 (10:00).....	Pointing
11 (13:00)–11 (17:00).....	Scan (path A)
11 (18:00)–12 (13:00).....	Pointing
12 (13:00)–12 (17:00).....	Scan (path A)
12 (18:00)–13 (21:30).....	Pointing
17 (12:30)–18 (06:00).....	Pointing
18 (11:00)–18 (14:30).....	Scan (path B)
18 (15:30)–19 (03:00).....	Pointing

Ginga satellite and the LAC are presented in separate papers (Makino and the ASTRO-C Team 1987; Turner et al. 1989). To determine the two-dimensional position in the 2–37 keV band and to search for a possible contaminating object near H0253+193, cross-scans were carried out. The field of view of the LAC is $1° \times 2°$ (FWHM) along and perpendicular to the scan path, respectively.

For spectral and timing studies, pointed observations were made for about 5 days in 1989 August, with a time span of 9 days as summarized in Table 1. The total effective exposure time was $\sim 7 \times 10^4$ s for the pointed observations.

3. RESULTS AND ANALYSIS

3.1. *Source Position*

We made scan profiles in the 2–10 keV band using the standard background subtraction method (Hayashida et al. 1989; Awaki et al. 1991). We applied a model fit for a point source convolved with the LAC collimator response. Two free parameters are allocated for the point source: one was the azimuthal position angle, and the other was the peak intensity. Using a fit model of the cross-scan profiles, we have determined the error region of the point source. The (α, δ) positions of the four corners of the error box for the 90% confidence level are (43°.22, 19°.21), (43°.31, 19°.29), (43°.35, 19°.18), and (43°.45, 19°.27), respectively. Within the error region, we relocated the *Einstein* IPC source H0253+193. The averaged intensity of the point source was about 10 counts s^{-1} (2–37 keV), or 1 mcrab.

3.2. *Orbital Variation of the X-Ray Spectra*

During the pointed observations, no X-ray source other than H0253+193 was found in the LAC field of view. The background subtraction for the pointed data was the same as that used for the scanning observation. The average X-ray intensity after the background subtraction was about 6 counts s^{-1} (2–10 keV), which is consistent with that of the scanning observation.

The X-ray light curve in the 2–20 keV energy band was presented in Paper I. We constructed the phase-resolved spectra and fitted them to the thermal bremsstrahlung model using the orbital period of 21,829 s given in Paper I. This model gave acceptable fits to most of the orbital-phase–resolved spectra. The best-fit parameters are potted in Figure 1 as a function of the orbital phase, where the heliocentric epoch is taken to be $1^h28^m15^s$ (UT) on 1989 August 11 (the eclipse center is defined as zero orbital phase). The average values of the temperature, iron line intensity, and iron line energy are 24 keV, 0.3 counts s^{-1}, and 6.7 keV, respectively. The mean X-ray luminosity in the 2–20 keV energy band at a distance of D pc is estimated to be 2×10^{31} ergs s^{-1} $(D/65 \text{ pc})^2$. The temperature ranged between 16 and 33 keV, although no systematic modulation with orbital phase was found. On the other hand, a remarkable orbital modulation was found in the N_H value. The variation of log N_H is well represented by a simple sinusoidal formula:

$$\log N_H = m_1 + m_2 \sin [2\pi(\text{orbital phase} + m_3)] , \quad (3.1)$$

where m_1, m_2, and m_3 are 22.9 ± 0.1, 0.15 ± 0.02, and 0.18 ± 0.02, respectively (errors quoted in this paper are single parameter at the 90% confidence level, unless specified). The resulting amplitude (maximum minus minimum) of N_H with orbital phase is 6×10^{22} cm^{-2}.

3.3. *Spectral Variation near the Eclipse*

We checked the X-ray data near the ingress and egress of the eclipse in more detail for spectral variations near the eclipse that may provide us with information on the X-ray–emitting region and companion star. An average transition curve during the ingress and egress was made by folding all of the available data with an orbital period of 21,829 s. The light curve and softness ratio (1.1–4.5 keV flux/4.5–9.2 keV flux) are given in Figure 2. The flux level during an eclipse is below the 0.3 counts s^{-1} detection limit, which is less than a few per cent of the normal level (noneclipse level). Therefore, the X-ray flux is completely or almost completely occulted during the eclipse. The transition time to the eclipse was estimated to about 100 s (see dashed line in Fig. 2). Within the relevant time bin of 32 s, we observed no change of the softness ratio during the ingress and egress of the eclipse.

3.4. *Pulse Profile*

The folded profiles with a 206 s pulse period are given in Figure 3 in three different energy bands. The pulse shapes are double-peaked in each energy band. Similar pulse shapes were found in previous observations made in 1987 and 1989 (Koyama et al. 1991). We defined the pulse modulation depth as (pulse peak count rate minus pulse bottom count rate)/(average count) in each energy band. To see the energy dependence of the amplitude, we plot these values against the incident photon energy as shown in Figure 4. A smaller pulse modulation is found at higher energy, while above 10 keV it becomes almost constant at less than 10%. These phenomena are similar to those in the other IPs (Norton & Watson 1989).

We have fitted the pulse-phase–resolved spectra with a thermal bremsstrahlung model. Although the fits are acceptable, the best-fit temperatures and N_H values show no systematic modulation with the pulse phase. We then fixed either the temperature or N_H to its mean value and again fitted the pulse-phase–resolved spectra. However, in these cases, we obtained no acceptable fit. Therefore, the pulse modulation is not solely due to a modulation of temperature or N_H value but would be due to a combined effect.

4. DISCUSSION

4.1. *Binary Parameters*

In Paper I crude estimates of the binary parameters of H0253+193 were given using the timing data of the orbital period and the durations of the eclipse and transition time to/from the eclipse. Here we will discuss the possibility that a self-consistent picture can be derived from a simple model of a white dwarf binary. Since the long-term X-ray luminosity has been almost constant, the mass accretion probably occurs as a

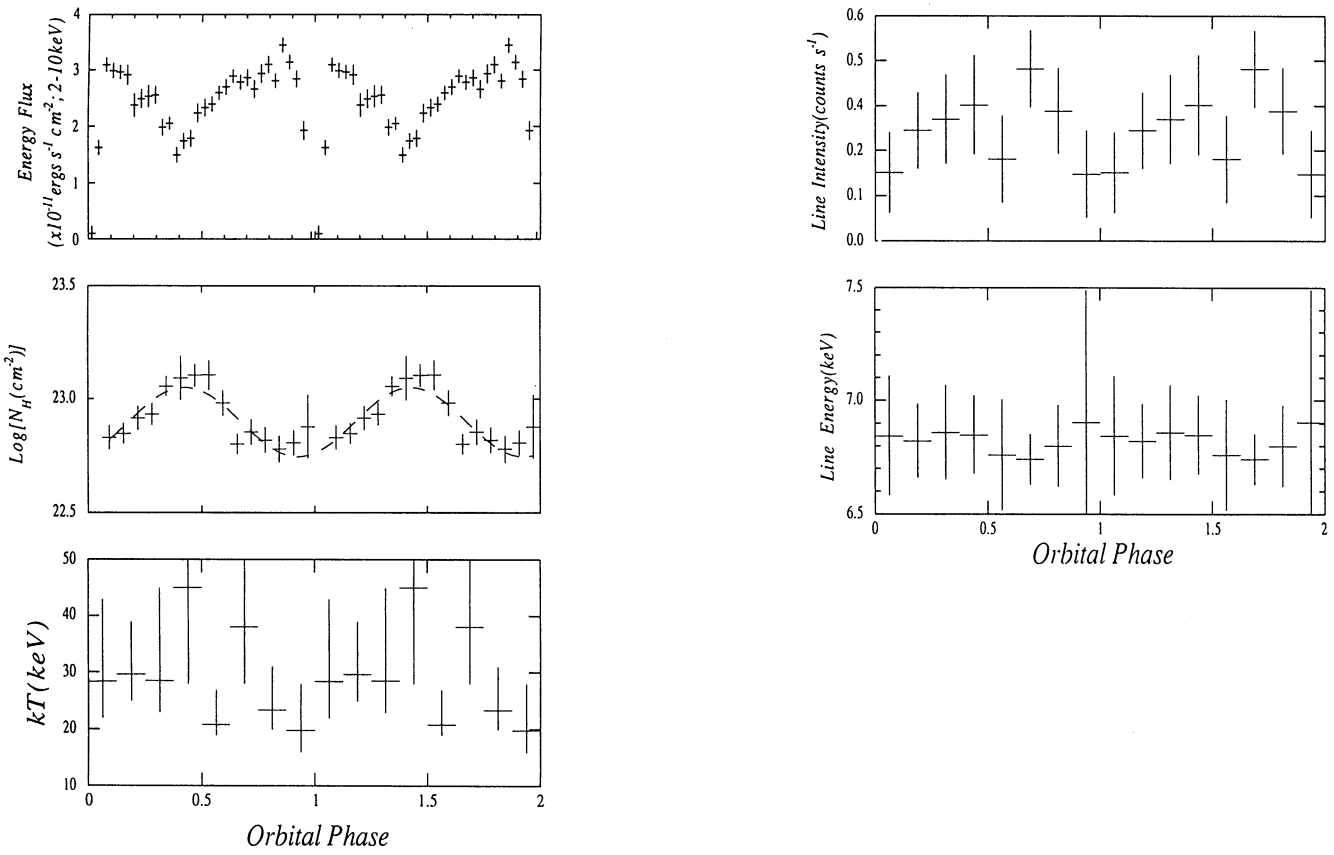

FIG. 1.—Best-fit parameter values with 90% confidence error are plotted as a function of orbital phase. The dashed lines are the best-fit values revealed by a χ^2 test (see text).

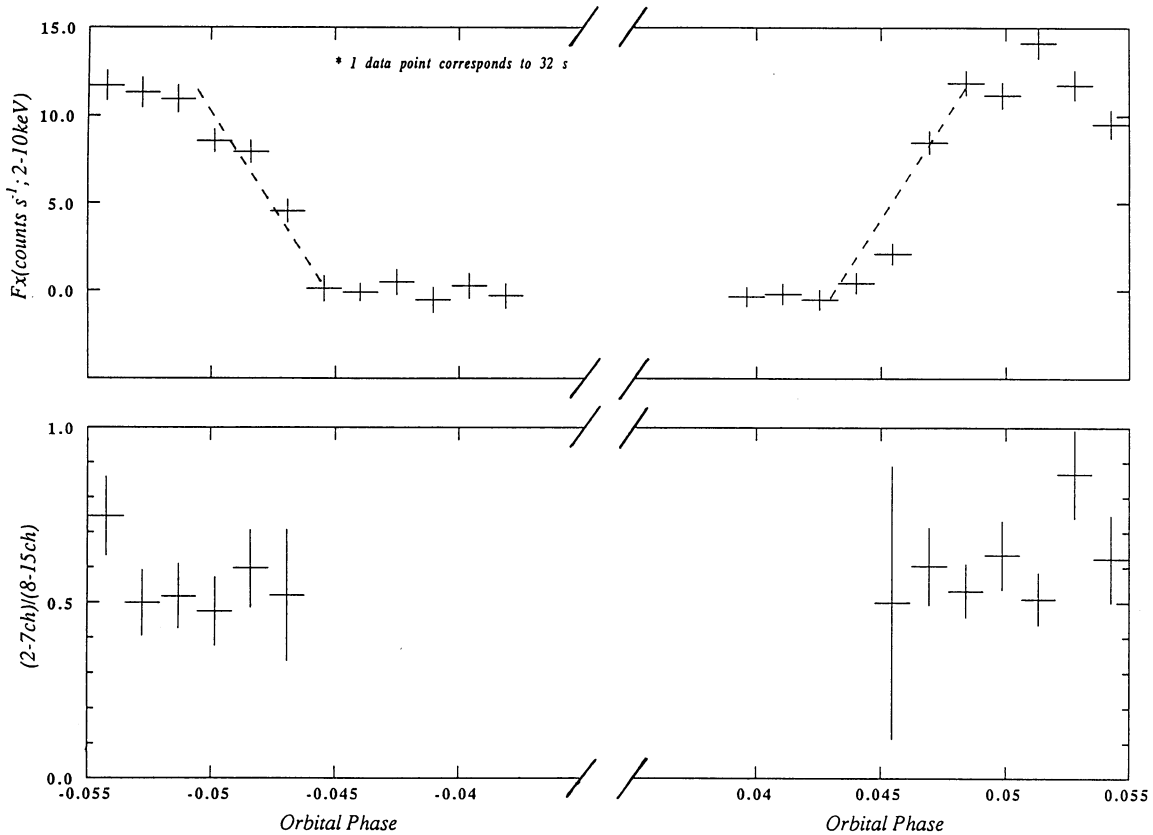

FIG. 2.—X-ray flux in the 2–10 keV energy band and the spectral softness ratio during the transition to and from eclipse. Errors are $\pm 1\ \sigma$. The dashed line is a visual aid only. The energy band (2–7 ch)/(8–15 ch) corresponds to (1.1–4.5 keV)/(4.5–9.2 keV) in the LAC.

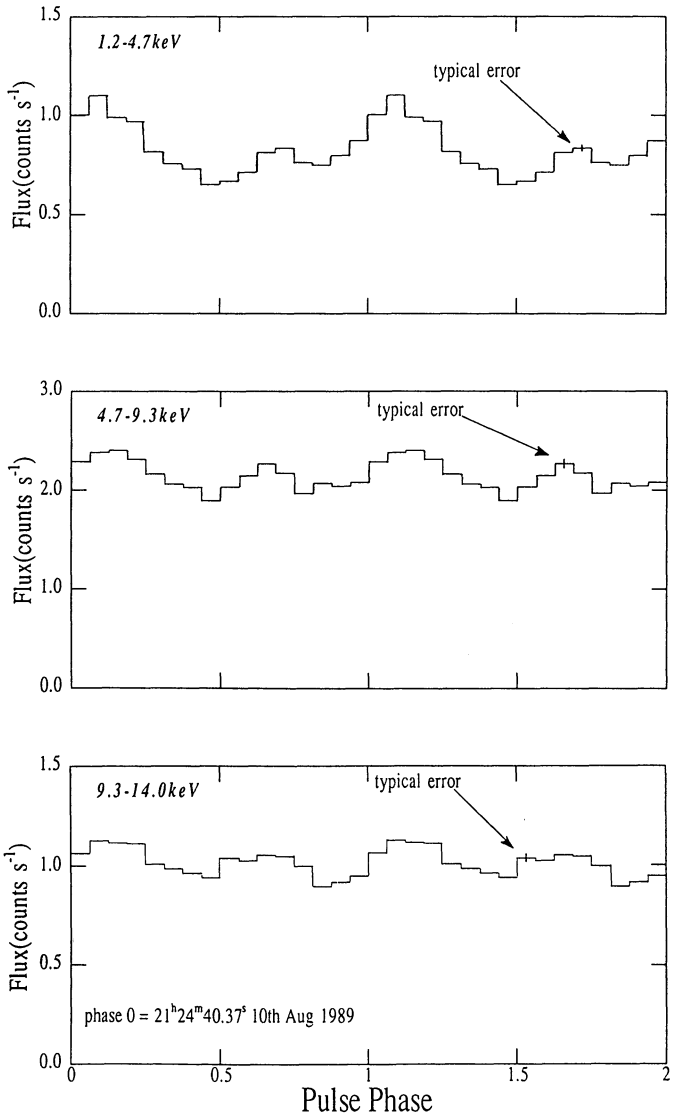

FIG. 3.—Pulse profiles in the three energy bands. All errors are defined as $\pm 1\,\sigma$.

result of Roche lobe overflow. For simplicity we will assume that the companion is a zero-age main-sequence (ZAMS) star, and the binary orbit is circular with the system inclination angle of 90°. From Kepler's third law, the orbital separation a is given by

$$a = 1.7\ R_\odot[(M_1 + M_2)/M_\odot]^{1/3}(P_{\rm orb}/6\ {\rm hr})^{1/3}\ , \qquad (4.1)$$

where M_1 and M_2 are masses of a white dwarf and a companion star, respectively.

Adopting an empirical mass-radius relation for the ZAMS companion and assuming that the radius of the Roche lobe is nearly equal to that of the companion, we obtained the mass and radius of the companion as follows (Patterson 1984):

$$M_2/M_\odot = 0.62(P_{\rm orb}/6\ {\rm hr})^{1.22}\ , \qquad (4.2)$$

$$R_2/R_\odot = 0.65(P_{\rm orb}/6\ {\rm hr})^{1.07}\ . \qquad (4.3)$$

We thus obtained the result that the mass and radius of the companion in H0253+193 are about 0.6 $M_\odot$ and 0.7 $R_\odot$, respectively.

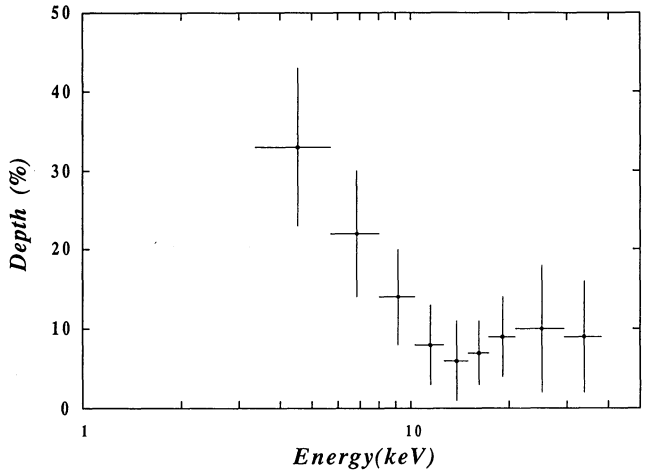

FIG. 4.—Energy dependence of the pulse modulation depth. The pulse modulation depth is defined as (pulse peak count rate minus pulse bottom count rate)/(pulse average count rate).

The mass of the white dwarf should be smaller than the Chandrasekhar limit 1.4 $M_\odot$, while that of the lower limit can be estimated assuming that the electron temperature of the X-ray–emitting plasma is less than that of a strong shock with a free-fall velocity at the white dwarf surface (Ishida 1992):

$$M_1 \geq 0.45(kT/20\ {\rm keV})^{3/4}\ M_\odot\ . \qquad (4.4)$$

Using the observed mean temperature, $kT = 24$ keV, we found that the lower limit of the white dwarf mass is about 0.5 $M_\odot$. Then the total mass of the binary system is 1.1–2.0 $M_\odot$, and hence, from equation (4.1), the orbital separation is 1.8–2.1 $R_\odot$.

Given the orbital separation a, we can estimate the radius of the companion star from the ratio of the eclipse duration and orbital period under the same assumption of a circular orbit with edge-on geometry. Since the eclipse duration is 9% of the orbital period, the radius of the companion star was estimated to be 0.5–0.6 $R_\odot$. This radius is roughly consistent with 0.7 $R_\odot$ derived from equation (4.2), giving support to the initial assumption of a Roche lobe overflow white dwarf binary model.

We have further analyzed the transition to and from eclipse, and found no spectral change during the transition, with a 32 s time bin. Since the pulsed fraction is small, we can assume that the intrinsic X-ray flux cannot change much during the eclipse transition. Thus, using the same discussion given in Paper I, we can estimate that the linear size of the X-ray–emitting region along the path of the orbital motion and the scale height of the stellar atmosphere of the companion star are (3–4) $\times$ 10^9 cm and less than about 10^9 cm, respectively. The small upper limit on the scale height of the companion star's atmosphere is consistent with a late-type main-sequence star. On the other hand, the linear size of the X-ray–emitting region seems extremely large: of the same order as, or even larger than, the radius of the typical white dwarf of (1–10) $\times$ 10^8 cm (Hamada & Salpeter 1961). Since the X-ray emission should be confined to a small region as a result of funneling of accreting matter by a possible strong magnetic field of the white dwarf, the reason for this rather large X-ray–emitting area is unknown.

4.2. *Accretion Flow*

Among the roughly one dozen previously studied X-ray–emitting IPs, only EX Hya shows an X-ray eclipse. Even in EX

Hya, the X-ray eclipse is partial. Most of the IPs have a single-peaked pulse profile (Norton & Watson 1989). On the other hand, H0253+193 exhibits a total eclipse in the X-ray band and a double-peaked pulse profile. Thus H0253+193 seems to be a rather "peculiar" IP. The apparent "peculiarity" of H0253+193 would not be intrinsic but would be due to a geometrical effect, because other important physical parameters of H0253+193, such as the X-ray spectrum (plasma temperature and iron line feature), the orbital and pulse periods, and the energy-dependent pulse modulation are typical among the IPs.

Since H0253+193 exhibits a clear total eclipse, the system is likely to have an edge-on geometry. The minimum N_H value was about 6×10^{22} cm^{-2}, which is still larger than that estimated from a radio observation (e.g., Koyama et al. 1991). Therefore, the location of the absorbing gas must be near the X-ray source. We found a sinusoidal modulation of log N_H with the orbital phase. This suggests that the overall structure of the absorbing gas is rather simple. The averaged N_H value of 8×10^{22} cm^{-2} is somewhat larger than that of typical IPs (e.g., Norton & Watson 1989). Therefore, the absorption is likely due to an accretion disk with a nearly grazing angle (edge-on geometry), so that a significant fraction of the accretion disk interposes on the line of sight to the white dwarf. However, we leave unexplained the fact that the larger amount of gas was found near the superior conjunction rather than the inferior conjunction of the white dwarf.

Hellier, Cropper, & Mason (1991) have proposed an "accretion curtain model" to explain the pulse modulation of EX Hya. In their model, the accretion disk is magnetically disrupted near the white dwarf and the accreting gas flows along the magnetic field lines. The spin modulation is caused by the change of absorption due to the optically thick accretion curtain as it rotates with the magnetic field line. This model may be applied to the pulse modulation of the other eclipsing binary H0253+193. However, there is a clear difference in pulse shape between H0253+193 and EX Hya (and other IPs): the former is double-peaked, while the latter is single-peaked. Therefore, the system geometry should be somewhat different. Since the two peaks of the pulse profile of H0253+193 have similar intensity, the two magnetic poles and associated magnetic field lines coming alternatively into our line of sight should have similar geometrical aspects. X-ray photons near the magnetic poles will be absorbed by the accreting gas along the field lines. Thus the largest photoelectric absorption occurs when the magnetic field line is near our line of sight. We have already suggested that the X-ray–emitting plasma has a large linear size. If this plasma has different temperatures at different positions, the observed temperature would be modulated as a result of self-occultation as the white dwarf rotates. In fact, the observations tend to support a combined effect of absorption and temperature changes.

5. CONCLUSION

1. We have determined the position of H0253+193 in the 2–20 keV energy band. The position determined by soft X-rays (0.3–3.5 keV range) with the *Einstein* IPC is within the error region.

2. The X-ray spectrum was well fitted by the thermal bremsstrahlung model with a temperature range of 16–33 keV, absorption (N_H) of $10^{22.5}$–$10^{23.2}$ cm^{-2}, and iron emission line at 6.7 ± 0.1 keV.

3. We found a sinusoidal variation of log N_H with orbital phase. The line-of-sight column density near the superior conjunction of the white dwarf is larger than that near the inferior conjunction.

4. H0253+193 exhibits a total eclipse, suggesting an edge-on geometry. No significant spectral variation during the eclipse transition was found, with a time resolution of 32 s.

5. The pulse shape of H0253+193 has a double-peaked structure. The pulse modulation is energy-dependent: the largest amplitude occurs at lowest energies. These phenomena are likely due to a combined effect of photoelectric absorption and self-occultation.

6. Assuming that H0253+193 is a Roche lobe overflow system with a circular orbit and edge-on geometry, we derived self-consistent binary parameters: the mass of the companion and white dwarf are 0.6 $M_\odot$ and ≥ 0.5 $M_\odot$, respectively; the linear size of the X-ray–emitting region, the radius of the companion star, and the orbital separation are estimated to be $(3–4) \times 10^9$ cm, 0.5–0.6 $R_\odot$ and 1.8–2.1 $R_\odot$, respectively; and the density scale height of the companion star is less than 10^9 cm.

The authors thank Y. Tawara for his contribution in the early stage of this work. We also thank S. Takano, K. Noguchi, H. Matsuhara, M. Ishida, and J. P. Osborne for their useful comments. J. Bock and S. Ran are greatly appreciated for their review of this manuscript. The data analysis was done with the M770 computer of the High Energy Laboratory of Nagoya University. The authors would like to thank Professor R. Kajikawa and all the members of the High Energy Laboratory.

REFERENCES

Awaki, H., Koyama, K., Kunieda, H., Takano, S., & Tawara, Y. 1991, ApJ, 366, 88
Clemens, D. P., & Leach, R. W. 1989, ApJ, 345, 346
Halpern, J. P., & Patterson, J. 1987, ApJ, 312, L31
Hamada, T., & Salpeter, E. E. 1961, ApJ, 134, 683
Hayashida, K., et al. 1989, PASJ, 41, 373
Hellier, C., Cropper, M., & Mason, K. O. 1991, MNRAS, 248, 233
Hobbs, L. M., Blitz, L., & Magnani, L. 1986, ApJ, 306, L109
Ishida, M. 1992, Ph.D. thesis, Tokyo Univ.
Kamata, Y., Tawara, Y., & Koyama, K. 1991, ApJ, 379, L65 (Paper I)
Koyama, K., et al. 1991, ApJ, 377, 240
Magnani, L., Blitz, L., & Mundy, L. 1985, ApJ, 295, 402
Makino, F., & the ASTRO-C Team. 1987, Astrophys. Lett. Comm., 25, 223
Norton, A. J., & Watson, M. G. 1989, MNRAS, 237, 853
Patterson, J. 1984, ApJS, 54, 443
Patterson, J., & Halpern, J. P. 1990, ApJ, 361, 173
Takano, S., Koyama, K., & Makishima, K. 1989a, PASJ, 41, 635
Takano, S., et al. 1989b, IAU Circ., No. 4745
Turner, M. J. L., et al. 1989, PASJ, 41, 345